Article

Not peer-reviewed version

A Patrol Route Design for Inclined Geosynchronous Orbit Satellites in Space Traffic Management

Ning Chen , Zhanyue Zhang , Songjiang Feng , Wu Xue , Boya Jia *

Posted Date: 10 February 2025

doi: 10.20944/preprints202502.0677.v1

Keywords: space traffic management; patrol constellation; IGSO; crossing points; spiral rings

Article

A Patrol Route Design for Inclined Geosynchronous Orbit Satellites in Space Traffic Management

Ning Chen, Zhanyue Zhang, Songjiang Feng, Wu Xue and Boya Jia *

Space Engineering University, China
* Correspondence: youxiang1445@qq.com

Abstract: Conducting survey and timely obtain of satellite status, especially for high-value GEO targets, is of great significance for Space Traffic Management. This article proposes an approach for patrolling Inclined Geosynchronous Orbit (IGSO) targets based on crossing points and spiral rings, which including six steps: (1) calculate the crossing position and crossing time of the IGSO targets; (2) design the spiral trajectory that satisfies desired patrol time; (3) divide IGSO targets into regions based on dichotomy approach; (4) calculate the bidirectional longitude drift rate within each region; (5) determine the starting position of patrol for each region; (6) determine the transfer trajectory for each region. On this basis, the proposed approach is analyzed and validated in detail. The results showed that the patrol orbit can effectively achieve patrol all of IGSO targets, with a period of no more than 40 days and an energy consumption of no more than 0.04km/s. And, the total energy consumption of a single patrol cycle in all regions shall not exceed 0.4km/s.

Keywords: space traffic management; patrol constellation; IGSO; crossing points; spiral rings

1. Introduction

Space activities, including not only commercial satellite launches and on-orbit service, but also space exploration missions by more and more countries and international organizations, are increasing day by day which has made space environment more complex. The importance of Space Traffic Management (STM) is becoming increasingly prominent. Space Traffic Management refers to the planning, supervision, coordination, and emergency response activities carried out by relevant management agencies through technical, legal, and other means to ensure the safe, efficient, and orderly launch, orbit operation, re-entry, and other activities of satellite, as well as to maintain the space environment and prevent unsafe factors such as electromagnetic interference, physical collisions, and environmental damage [1–4].

Space Traffic Management revolves around three core goals: safety, orderliness, and sustainability. Safety is primary consideration, which means ensuring the normal operation of satellite and related equipment, and preventing the occurrence of various accidents and incidents. As an important component of Space Traffic Management, the Space Situational Awareness (SSA) system is primarily responsible for monitoring and tracking of space targets, ensuring the safety and sustainable use of the space environment. In the vast expanse of space, GEO Zone is a key area for Space Traffic Management. It is generally considered that the GEO is a circular orbit with inclination of 0° and earth-radius of 42164km. In a strict sense, there is only one GEO in space. In order to effectively use and protect GEO, Inter-Agency Space Debris Coordination Committee (IADC) has artificially delineated a GEO Zone as shown in Figure 1 [5]. It can be seen that the GEO Zone's upper and lower height is 35786km±200km, and the north-south range is latitude ±15°. In the Zone, the inner ±75km zone is GEO working zone while the rest is GEO maneuver zone. Satellites in GEO Zone are widely used in navigation, communication, early warning and other fields due the unique orbital advantage, such as the sub-satellite point trajectory and global coverage [6].

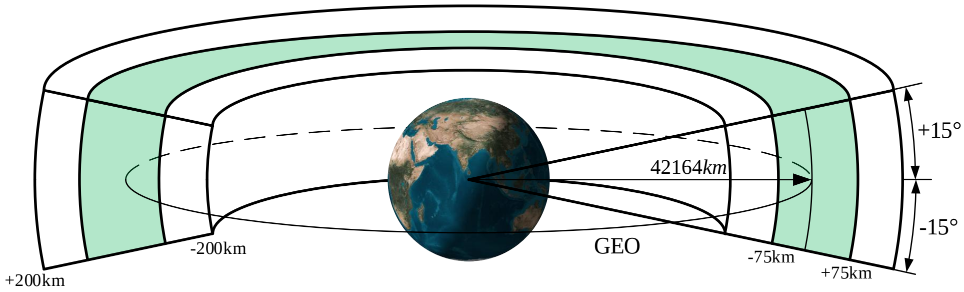

Figure 1. GEO Zone Defined by IADC.

The prerequisite for Space Traffic Management in GEO is to obtain the status information of GEO targets quickly and accurately. However, due to the long distance and poor tracking accuracy, the ground-based space situation awareness system for GEO satellites inspection is limited. Space-based observation, which can achieve close range, long-term, and multi-angle tracking and observation of space targets, becomes the only means to obtain detailed information of GEO satellite. Due to the vastness of GEO, GEO SSA typically adopts a method of traverse patrol, which is similar to traffic patrol, called Space Traffic Patrol. Space Traffic Patrol means to go around a Zone or an area at regular times to check that it is safe and that there is no trouble at close range by using one or more satellite.

According to the UCS database, as of May 2023, there are 590 controllable GEO satellites [7]. In terms of satellite types, GEO satellites can be divided into three categories: military, civilian/government, and commercial. The number of commercial satellites is largest, accounting for about 57%, and the military and civilian/government is equivalent, accounting for 21% and 22%. When considering that the perigee and apogee are both in working zone, the number of qualified satellites are 495, accounting for about 84%. When considering the distribution of orbital inclination, it can be seen that although most GEO satellites have a small inclination angle, but the number of satellite inclinations exceed 0.1° is 179, accounting for more than 30%. Those satellites belong to a different orbital plane from the patrol satellite due to its inclination, which poses a huge challenge to Space Traffic Patrol. In this article, we define an inclined geosynchronous orbit (IGSO) target is a satellite with inclination angle exceed 0.1°.

Essentially, the Space Traffic Patrol problem belongs to the problem of multiple targets rendezvous. There are a lot of domestic and international researchers who engage in it, especially in terms of On-Orbit-Services. Those articles can be divided into four categories: One-to-Multiple (OTM), Multiple-to-Multiple (MTM), Peer-to-Peer (PTP), and Mixed.

OTM means that one service satellite refuels multiple targets. In OTM, most scholars consider service order as the main variable for optimization, with the minimum consumption as the optimization objective. Those scholars transform it into a Travel Salesman Problem (TSP) or a Mixed Integer Nonlinear Programming (MILP) problem. Ref. [8] studied the OTM service order problem with the service satellite and targets in same circular orbit. Ref. [9] studied the route problem of servicing GEO targets with small inclination, while same question as in Ref. [10]. In addition, a spiral cruise orbit for GEO satellites traverse was designed by using relative orbit equations in Ref. [11,12]. Genetic algorithms (GA), Particle Swarm Optimization (PSO) and other optimization algorithms are also used to solve the problem [13–18].

MTM means that multiple service satellites refuel multiple targets. MTM problem is much more complex than OTM. Many factors, such as initial position and traverse cost, will affect the path planning. Moreover, considering the limited capacity of service satellite, it is necessary to place the location and number of fuel stations to affect the final result. For MTM, different scenarios are set and different models are established. Ref. [19] assumes that the service satellite can return to fuel station for refueling and continue the service. Taking the service sequence and the time of return to station as variables, the service plan with lowest consumption is optimized. By converting the problem into a Location-Route Problem (LRP), a service plan is given in Ref. [20], same as in Ref [25–29]. Some

Preprints.org (www.preprints.org) | NOT PEER-REVIEWED | Posted: 10 February 2025 doi:10.20944/preprints202502.0677.v1

others solved the problem by converting it into an Optimal Matching Problem (OMP) [21,22] or a mixed mode [23,24].

PTP assumes that each service satellite and target have the ability to maneuver. PTP is actually an optimal matching problem, and the model is established depending on the constraints of the scene conditions. All models were varying slightly. To make all targets fuel-abundant with lowest cost, the PTP problem was transformed into an optimal matching problem model and solved by using auction algorithms. Ref. [30] studied the PTP traverse mode assuming that targets in a circular orbit with uneven fuel distribution. The PTP refueling model added fuel quantity threshold as a new parameter, where targets with larger quantity as fuel-abundant and smaller quantity as fuel deficient [31]. Furthermore, some scholars assumed that each service satellite can return to the original position of anyone after rendezvous, transformed it into a three-index assignment problem, also called E-PTP (Egalitarian Peer to Peer) problem, and solved it by using search algorithms [32].

Mixed traverse is relatively complex, and generally two or more categories are used to achieve the goal of reducing fuel consumption or more effective traverse. Ref. [33–35] simplifies the MTM and PTP to achieve equilibrium through weighting, resulting in a relatively ideal state for fuel consumption and fuel gap between targets. Ref. [36] selected some service satellites to only provide fuel for some targets in the constellation. After these targets receive fuel, they transform into service satellites to provide fuel for other targets. Through enumeration and PSO comprehensive algorithm comparison, it was verified that the hybrid traverse strategy is more cost-effective than other strategies.

Although there are many literature studies on this topic, most of them focus on the coplanar rendezvous, and there is relatively little research on non-coplanar rendezvous problem. Bai et al. used the dual target rendezvous orbit cluster to obtain the rendezvous orbit approaching multiple non-coplanar targets by searching and calculating the closest distance to other targets [37–39]. Zhang et al. used Lambert's theorem to determine the service satellite orbit that were close to two targets, and then improved the orbit by using least squares method and genetic algorithm, obtained the orbit that approaches three non-coplanar targets [40–42]. Ref [43] demonstrated a service satellite orbit that can rendezvous with multiple satellites in Walker constellation without orbit maneuver. Based on this, the author summarized the rendezvous orbit constraints for maximum number of constellation satellites, and then used phase modulation to change the initial phase of service satellite to rendezvous with all satellites in the orbit plane. The strategy is verified that fuel consumption is less compared to the Lambert's theorem. Mana et al. designed the traversal orbit for GPS satellites by using single pulse coplanar orbit maneuver. After traversing one orbit plane, the maneuver is carried out at the intersection with next one, and repeating the same operation until the traversal of all satellites [44].

The above articles mainly focus on Walker constellation, but IGSO orbit is not a regular Walker constellation, but rather an irregular problem. To solve the rendezvous multiple targets problem on general orbital plane, Zhang et al. proposed the crossing point method, and achieving the rendezvous orbit based on the method [45–47].

In this article, we propose a patrol route design approach based on gradient longitude drift rate and crossing points to patrol IGSO targets. Sec. II introduces the approach in detail. And, the proposed approach is illustrated in Sec. III by using numerical experiment. Additionally, the discussion is illustrated in Section IV. Finally, the conclusion and future work directions are provided in Section V.

2. Materials and Methods

For safety, the patrol satellite should not frequently pass through the GEO working zone, and not affect the normal satellites in working zone. Thus, the patrol satellite should be located in GEO maneuver zone defined by IADC. It can be seen from the definition that the GEO maneuver zone is divided into two in-dependent parts, above or below GEO. Therefore, the patrol orbit zone should be located in a part of the maneuver zone. When the satellite is in the maneuver zone, it will drift

Preprints.org (www.preprints.org) | NOT PEER-REVIEWED | Posted: 10 February 2025 doi:10.20944/preprints202502.0677.v1

relative to GEO. Taking the standard GEO as the reference coordinate system, the patrol route relative to the GEO is shown in Figure 2.

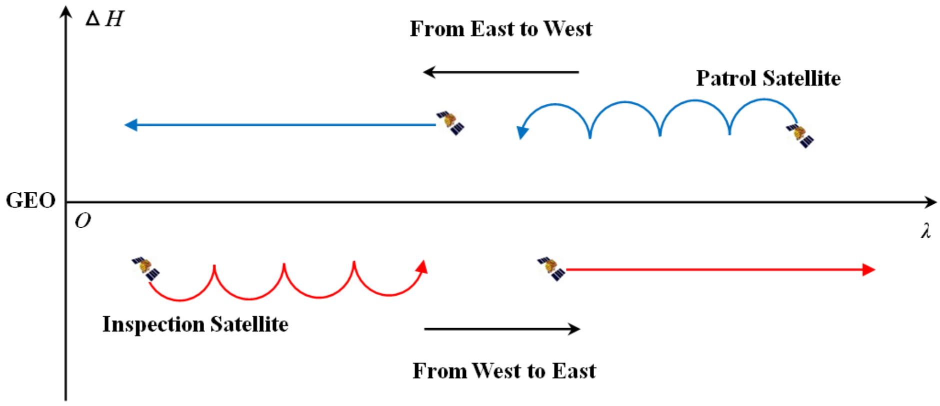

Figure 2. Patrol route relative to GEO orbit.

It can be seen from the figure that when the satellite is located below GEO, its trajectory relative to GEO is wave-shaped (elliptical orbit) or linear (circular orbit). The sub-satellite point longitude becomes larger, and drifts from west to east. Conversely, when located above the GEO, its relative trajectory is also wave or linear with sub-satellite point longitude becomes smaller and drifts from east to west.

By utilizing the relative drift, it is possible to patrol the GEO targets. The longitude drift rate D is

$$D = -0.0128(a - a_c) \quad (1)$$

Therefore, by designing drift rate reasonably, it is possible to achieve a natural patrol of all targets in GEO zone. As shown in Figure 3, assume that a GEO zone contains six targets. The patrol satellite first drifts from west to east, observing target 2 and 6 at apogee, and then implementing orbital maneuver at the zone boundary, turn around and drifts from east to west, observing target 1, 3, 4, and 5 at perigee. Thereby, the satellite achieves the patrol of the entire zone's targets. Afterwards, through orbital maneuver, the satellite will turn around again and enter the East-Drift orbit, conducting periodic patrol of targets in the zone.

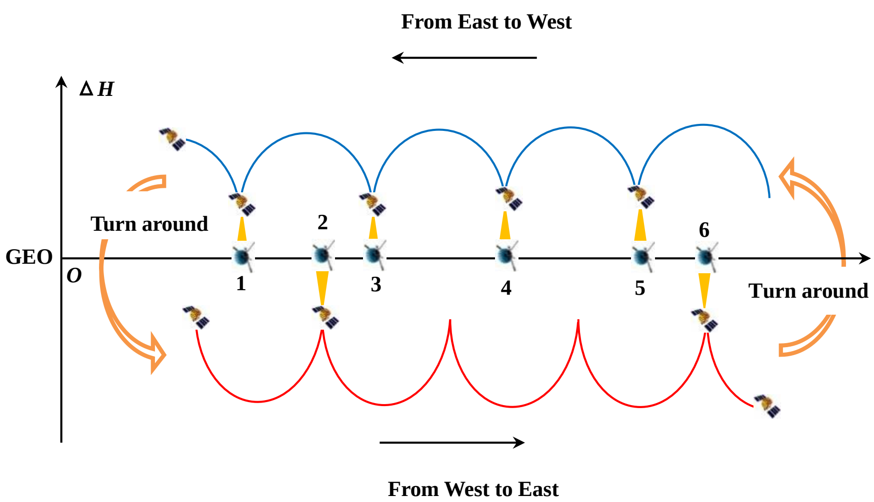

Figure 3. Schematic diagram of patrol strategy.

Preprints.org (www.preprints.org) | NOT PEER-REVIEWED | Posted: 10 February 2025 doi:10.20944/preprints202502.0677.v1

The above strategy is very effective when the target is stationary, but IGSO targets exhibit up and down relative to the equatorial plane. Patrolling these targets not only requires consideration of relative position, but also relative time, which is a more complex spatiotemporal problem. According to orbital dynamics, each satellite is in a plane passing through the center of Earth. That is, the orbital planes of any two satellites will inevitably intersect, forming two intersection points, called crossing points, as shown in the following Figure 4.

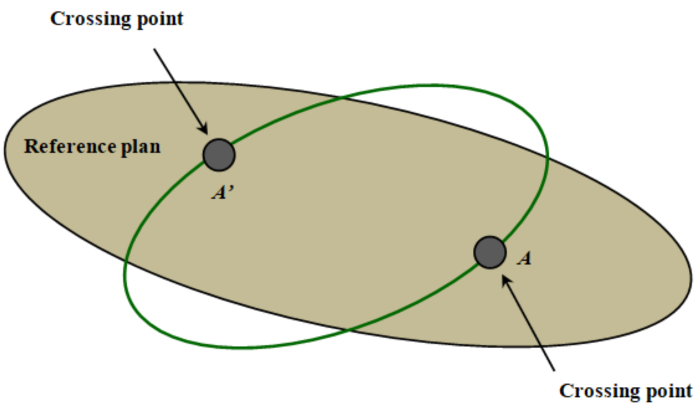

Figure 4. Schematic diagram of satellite crossing point.

Select any orbit plane as the reference plane, and the target orbit passes through the reference plane and intersects at points A and A', where point A north of the equatorial plane is called the north crossing point, and point A' south of the equatorial plane is called the south crossing point. The two points have a phase difference of 180 ° within the reference plane.

If we use the strategy above to implement the patrol of IGSO targets, there will be a situation where the patrol satellite nears the crossing point, but the target does not reach the crossing point. If the patrol satellite could hold on near the crossing point for a period of time, waiting the target crosses the reference plane, then the problem can be smoothly transformed into the stationary problem. According to the space special orbit design theory [47], when the height difference meets certain conditions, it can achieve a spiral holding-on effect as shown in Figure5.

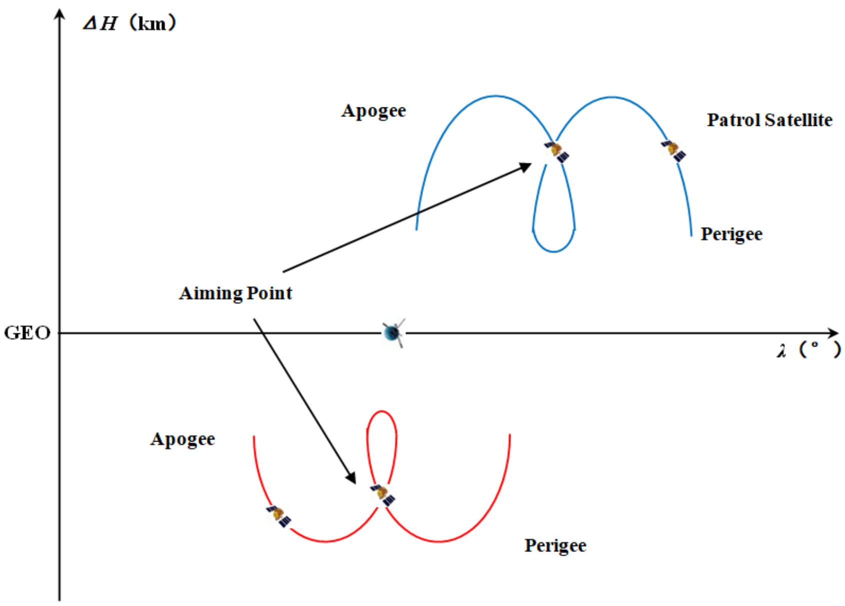

Figure 5. Schematic diagram of spiral cruise.

Preprints.org (www.preprints.org) | NOT PEER-REVIEWED | Posted: 10 February 2025 doi:10.20944/preprints202502.0677.v1

When the target crosses the reference plane, the patrol satellite happens to be on the spiral ring. By designing the spiral ring reasonably, the cycle of the spiral ring can cover the crossing time within a day. This transforms the patrol problem of IGSO targets into a stationary target problem, and uses the gradient longitude drift rate method to achieve patrol of IGSO targets.

This article proposes a gradient longitude drift rate patrol configuration approach based on crossing points and spiral rings to patrol IGSO targets, includes:

(1) Calculate the crossing position and crossing time of the IGSO targets;
(2) Design the spiral trajectory that satisfies desired patrol time;
(3) Divide IGSO targets into regions based on dichotomy approach;
(4) Calculate the bidirectional longitude drift rate within each region;
(5) Determine the starting position of patrol for each region;
(6) Determine the transfer trajectory for each region.

2.1. Calculate the Crossing Position and Crossing Time of the igso Targets

Assuming a IGSO target crosses the orbital plane, the target orbital element is $(a_t, e_t, i_t, \Omega_t, \omega_t, \tau_t)$. Set the orbital plane of patrol satellite as reference plane, which can be represented by (i_s, Ω_s). The coordinates of crossing point in reference plane can be represented as (t, r, ϕ), where t is the moment when target crosses through the plane, r is the geocentric distance of the crossing point, and ϕ is the ascending intersection angle of the crossing point. If crossing point is (t_N, r_N, ϕ_N), thus

$$\begin{aligned} \cos\phi_N &= \cos(\Omega_t - \Omega_s)\cos u_N + \sin u_N \sin(\Omega_t - \Omega_s)\cos(180^\circ - i_t) \\ \sin\phi_N &= \frac{\sin u_N \sin i_t}{\sin i_s} = \frac{\sin(\Omega_t - \Omega_s)\sin i_t}{\sin(i_t - i_s)} \end{aligned} \tag{2}$$

Among them, u_N is the argument of latitude of the target, which can be obtained by

$$tg\phi_N = \frac{\sin(\Omega_t - \Omega_S)}{\cos(\Omega_t - \Omega_s)\cos i_s + \sin i_s ctg(180^\circ - i_t)} \tag{3}$$

The crossing time can be obtained from the Kepler equation:

$$t_N = (E_N - e_t \sin E_N)\sqrt{\frac{a_t^3}{\mu}} + \tau_t \tag{4}$$

$$tg\frac{E_N}{2} = \sqrt{\frac{1-e_t}{1+e_t}}\, tg\frac{(u_N - \omega_t)}{2} \tag{5}$$

The south crossing point and north crossing point are symmetrical relative to the center of the earth, then the south crossing point (t_S, r_S, ϕ_S) is

$$\begin{cases} t_S = (E_S - e_t \sin E_S)\sqrt{\dfrac{a_t^3}{\mu}} + \tau_t \\ \phi_S = \pi + \phi_N \\ r_S = \dfrac{a_t(1-e_t^2)}{1+e_t\cos(u_S - \omega_t)} \end{cases} \tag{6}$$

Due to the periodic motion, the target periodically crosses the reference plane, with a time interval of orbital period T_t , i.e

$$\begin{cases} t_{mN} = t_N + mT_t \\ t_{mS} = t_S + mT_t \end{cases} \qquad m = 0,1,2,\cdots \tag{7}$$

In this article, the patrol satellite operates within the equatorial plane, thus

$$\begin{aligned} i_s &= 0 \\ \Omega_s &= 0 \end{aligned} \tag{8}$$

Then, the crossing point becomes the ascending and descending node of target, and the crossing point can be represented by (t,Ω). Thus, formulas (5)~(8) derive the crossing time as

$$t_{mN} = (E_N - e_t \sin E_N)\sqrt{\frac{a_t^3}{\mu}} + \tau_t + 2\pi m\sqrt{\frac{a_t^3}{\mu}} \qquad m = 0,1,2,\cdots \tag{9}$$

Considering that most IGSO targets is in near circular orbit, thus

$$\begin{aligned} E &\approx M \approx f \\ e &\approx 0 \end{aligned} \tag{10}$$

Formula (9) can be simplified as:

$$\begin{aligned} \frac{dt_{mN}}{dt} &= \frac{d(E_N + 2\pi m)}{dt}\sqrt{\frac{a_t^3}{\mu}} + (E_N + 2\pi m)\frac{d\sqrt{\frac{a_t^3}{\mu}}}{dt} \\ &= \frac{dE_N}{dt}\sqrt{\frac{a_t^3}{\mu}} + \frac{3}{2}(E_N + 2\pi m)\sqrt{\frac{a_t}{\mu}}\frac{da}{dt} \\ &= \frac{d\lambda}{dt}\sqrt{\frac{a_t^3}{\mu}} + \frac{3}{2}\frac{(E_N + 2\pi m)}{a_t}\sqrt{\frac{a_t^3}{\mu}}\frac{da}{dt} \approx -\frac{3}{2a_c}(a_t - a_c) \end{aligned} \tag{11}$$

a_c is the radius of geostationary orbit. It can be seen that the change of crossing time is closely related to the semi major axis difference between target and a_c. The difference between two consecutive crossing times is

$$\begin{aligned} \Delta t_N &= -\frac{3}{2a_c}(a_t - a_c)2\pi\sqrt{\frac{a_t^3}{\mu}} \\ &= 2\pi\sqrt{\frac{a_c^3}{\mu}}\left(-\frac{3}{2a_c}(a_t - a_c)\sqrt{\frac{a_t^3}{a_c^3}}\right) \\ &= -\frac{3}{2a_c}(a_t - a_c)T_e \end{aligned} \tag{12}$$

If the semi major axis difference is 100km, it can be obtained that the daily variation of crossing time is about 306.5 seconds. Considering that the semi major axis change is only a few kilometers under the perturbation, it can be considered that the crossing time of IGSO target in this article remains basically unchanged. The Ω will also experience precession drift due to the perturbation influence, and the drift pattern is as follows

$$\Omega = \Omega_0 + \left(K_{i1}\pi + \frac{3\pi}{4}\left(\frac{\omega_s}{n}\right)^2\left(1 - \frac{\cos 2\xi_s}{2}\right) + \frac{3\pi}{4}\left(\frac{\omega_m}{n}\right)^2\left(1 - \frac{\cos 2\xi_m}{2}\right)\right)t \tag{13}$$

It can be obtained that the Ω decreases by about 0.0089 ° per day. However, under controlled conditions, the Ω will remain within ± 0.1 ° of its sub-point longitude. Therefore, in this paper, we consider that the crossing points of selected targets remain unchanged.

2.2. Design the Spiral Trajectory That Satisfies Desired Patrol Time

As shown in Figure5, the intersection point is called aiming point, and the point where the trajectory turns from west to east or from east to west is called turning point. Satellite passes through the same aiming point twice is called a spiral loop, which is a closed teardrop trajectory relative to

Preprints.org (www.preprints.org) | NOT PEER-REVIEWED | Posted: 10 February 2025 doi:10.20944/preprints202502.0677.v1

GEO. The turning point is the point where the velocity of patrol satellite is equal to the GEO. Using the vitality formula, turning point is

$$v^2 = \frac{2\mu}{r} - \frac{\mu}{a} = \frac{\mu}{a_c} \tag{14}$$

Among them, v is the velocity of the turning point, a is the semi major axis of the patrol satellite, r is the position of the turning point, and μ is the gravitational constant of the Earth. The turning point position is

$$r = \frac{2aa_c}{a_c + a} \tag{15}$$

According to the displacement difference between aiming point and turning point, it is approximately equal to half of the difference between the aiming point and the satellite, that is, the position of the aiming point is

$$R = \begin{cases} 2r + 75 - a_c & r < a_c \\ 2r - 75 - a_c & r > a_c \end{cases} \tag{16}$$

The period of the spiral ring is the time interval where the satellite continuously passing through the same aiming point, which is approximately twice the time between turning points. Similarly, it can be obtained that:

$$T_s \approx 4\sqrt{\frac{a^3}{\mu}}\left(\arccos\left(\frac{1-v_s}{e}\right) + e\sin\left(\arccos\left(\frac{1-v_s}{e}\right)\right)\right) \tag{17}$$

where v_s is the energy parameter at the turning point, which is:

$$v_s = \frac{v^2}{\frac{\mu}{r}} = \frac{\frac{\mu}{a_c}}{\frac{\mu}{r}} = \frac{r}{a_c} = \frac{2a}{a_c + a} \tag{18}$$

Assuming that the crossing times within a day is $\{T_1,T_2,\ldots,T_n\}$, and the earliest aiming point is T_{ins}, thus.

$$\begin{aligned} T_s &\geq \max\{T_i\} - \min\{T_i\} \\ T_{ins} &= \min\{T_i\} \end{aligned} \tag{19}$$

2.3. Divide IGSO Targets into Regions Based on Dichotomy Approach

It can be seen that when the longitude drift rate is constant, the patrol period of targets depends on the maximum longitude difference. On the other hand, if the distribution of longitude differences between targets within the zone is uneven, there will be a situation where the targets are concentrated on both sides, which causes a great waste of time. Therefore, when designing the patrol configuration, it is necessary to consider dividing all targets reasonably to ensure that the longitude differences within each zone are consistent, so that the patrol periods of each zone are not significantly different, and thus achieve periodic patrol of all targets.

Without losing generality, sort n GEO targets in ascending order according to their sub-satellite point longitude, and record the longitude as λ_i (i=1, 2,..., n), and $\lambda_1 < \lambda_2 < \ldots < \lambda_n$. Distributed on GEO orbits, the difference in longitude between adjacent targets is recorded as $\Delta\lambda_i$ (i=1, 2,..., n), then there is

$$\begin{aligned} \Delta\lambda_i &= \lambda_{i+1} - \lambda_i \quad i = 1\cdots n-1 \\ \Delta\lambda_n &= \lambda_1 - \lambda_n + 360 \end{aligned} \tag{20}$$

 doi:10.20944/preprints202502.0677.v1

When the distribution of GEO targets is uneven, there will inevitably be several large longitude gaps. If the divided area covers the gaps, there will be a significant in-crease in patrol period due to a single target. Therefore, when dividing zones, it is necessary to avoid these huge gaps as much as possible.

This paper presents a zone division method based on dichotomy approach, which can quickly perform zone division. Set the maximum and second largest longitude difference gap between targets as

$$\begin{aligned} \Delta\lambda_{\max} &= \max\left\{\Delta\lambda_i\right\} \quad i = 1\cdots n \\ \Delta\lambda_{\sec-\max} &= \max\left\{\left\langle \Delta\lambda_i \middle| \Delta\lambda_{\max}\right\rangle\right\} \quad i = 1\cdots n \end{aligned} \tag{21}$$

Due to the characteristic of circular distribution, these two longitude differences divide all targets into two zones, as shown in Figure 6.

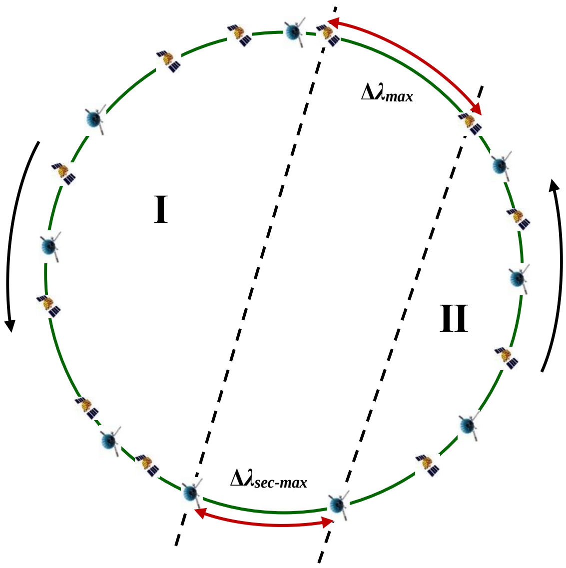

Figure 6. Schematic diagram of zone division.

The longitude coverage ranges of the two zones are

$$\begin{aligned} &\mathrm{I} \quad \lambda_{\max+1} \sim \lambda_{\sec-\max} \\ &\mathrm{II} \quad \lambda_{\sec-\max+1} \sim \lambda_{\max} \end{aligned} \tag{22}$$

Set the range of longitude drift rate to

$$D \subseteq \left\{D_{\min} \sim D_{\max}\right\} \tag{23}$$

Then the maximum patrol period of the two zones can be calculated as

$$\begin{aligned} T_{\mathrm{I}} &= \frac{\lambda_{\sec-\max} + 360 - \lambda_{\max+1}}{D_{\min}} \\ T_{\mathrm{II}} &= \frac{\lambda_{\max} - \lambda_{\sec-\max+1}}{D_{\min}} \end{aligned} \tag{24}$$

Compare the sizes of T_{I} and T_{II}, select the zone with a larger period, select the maximum longitude difference gap within the zone, and perform secondary division, as shown in Figure 7.

Preprints.org (www.preprints.org) | NOT PEER-REVIEWED | Posted: 10 February 2025 doi:10.20944/preprints202502.0677.v1

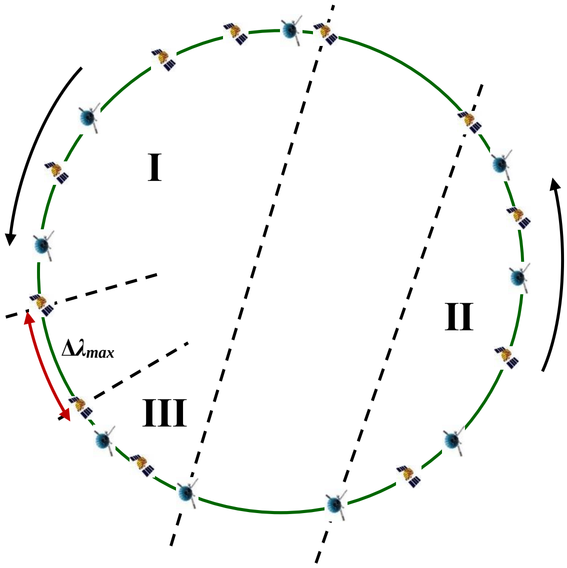

Figure 7. Schematic diagram of second zone division.

Compare the periods of the three zones T_I , T_{II} and T_{III}, and also select the zones with larger periods for segmentation using the maximum longitude difference gap until all zones meet the patrol period T_0 (T_0 is the given limitation period), as shown in Figure 8.

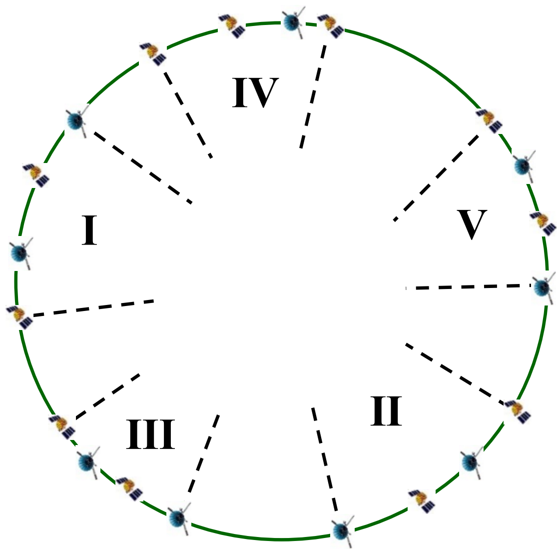

Figure 8. Schematic diagram of zone division result.

The process steps for dividing the entire zone are shown in Figure 9.

 doi:10.20944/preprints202502.0677.v1

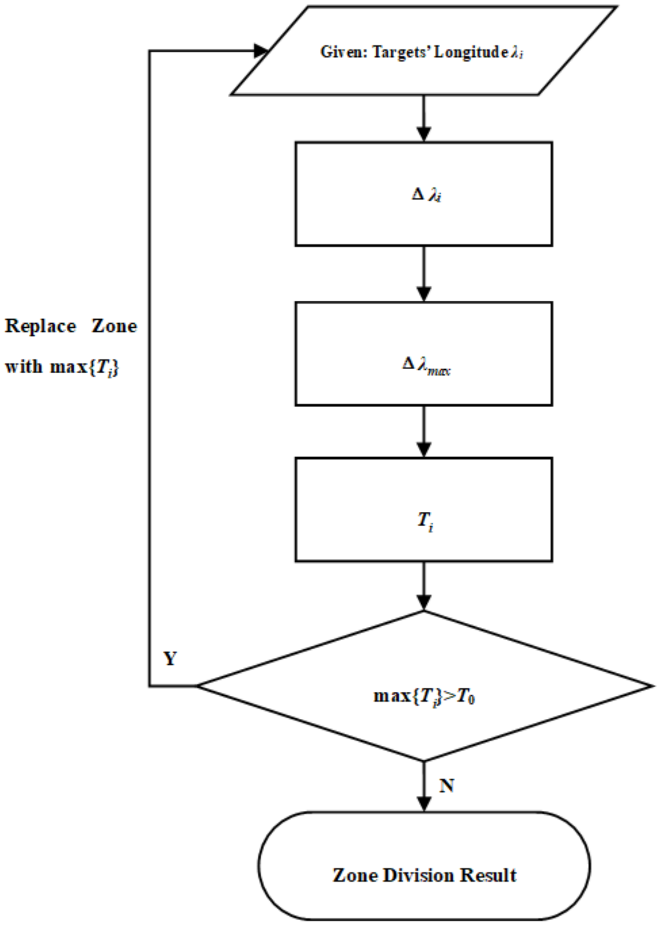

Figure 9. Zone division process.

2.4. Calculate the Bidirectional Longitude Drift Rate within Each Region

After dividing the entire target into multiple zones, it is necessary to determine the east/west longitude drift rate within each zone. Assuming n targets are divided into N zones, denoted as Z_i (i=1, 2, ..., N), each zone contains M_i targets, represented by their sub-satellite point longitude, denoted as λ_{ij} (i=1, 2, ..., N, j=1, 2, ..., M_i). Thus

$$\begin{aligned} &Z_i = \{\lambda_{i1} \quad \lambda_{i2} \quad \cdots \quad \lambda_{iM_i}\} \\ &\sum_{i=1}^{N} M_i = n \end{aligned} \tag{25}$$

It can be seen from Figure 4 that if target k and target l can be observed in one patrol, their longitude difference needs to be an integral multiple of the drift rate, which is

$$|\lambda_k - \lambda_l| = pD \quad p \in N \tag{26}$$

The above equation also indicates that the remainder of t drift rate D for target k and target l is the same, which is

$$\mathrm{mod}(\lambda_k \quad D) = \mathrm{mod}(\lambda_l \quad D) \tag{27}$$

Assuming that the eastward longitude drift rate of the patrol satellite is D_E and the westward is D_W. It can be inferred from the above analysis that the conditions for achieving patrol of targets can be transformed into the existence of D_E and D_W, so that the eastward target set Q_E with the same remainder of D_E, and the westward target set Q_W with the same remainder of D_W, meet the union of the Q_E and Q_W can include all targets

Preprints.org (www.preprints.org) | NOT PEER-REVIEWED | Posted: 10 February 2025 doi:10.20944/preprints202502.0677.v1

$$Z = Q_E \cup Q_W \tag{28}$$

Taking zone N as an example for analysis, the sub-satellite point longitude of the targets is λ_j (j=1, 2, ..., M_N). Considering the existence of the GEO satellite box, keep the sub-satellite point to one decimal, denoted as λ_j^* (j=1, 2, ..., M_N). Simultaneously, simplify the longitude drift rate to one decimal

$$D \subseteq \{D_1 \quad D_2 \quad \cdots \quad D_d\} \tag{29}$$

order

$$q_{D_i} = \{\mathrm{mod}(\lambda_j^* \quad D_i)\} \tag{30}$$

Take Q corresponding to the mode of the above set, denoted as Q_{Di}, then

$$Q_{D_i} = \{\lambda_j | \mathrm{mod}(\lambda_j^* \quad D_i) = MODE(q_{D_i})\} \tag{31}$$

Join the above target sets until patrol of all targets is achieved

$$Z_N = Q_{D_k} \cup Q_{D_l} \tag{32}$$

Considering that the orbital periods for patrol satellite are not significantly different, the drift rate affects the number of patrol cycles under certain longitude difference conditions. The larger the drift rate, the more longitudes drift each day, the fewer cycles required for patrol, and the shorter the corresponding patrol cycle. On the contrary, the smaller the drift rate, the longer the patrol period. Therefore, patrol satellites with high longitude drift rates should be selected firstly. When satellites with high longitude drift rates do not meet the requirements for patrol, they choose to use smaller longitude drift rates for patrol.

In addition, according to the constraint analysis, there is redundancy in the observation distance. By adjusting the observation distance, a certain sub-satellite point longitude threshold can be brought to the target's sub-satellite point longitude, as shown in Figure 10.

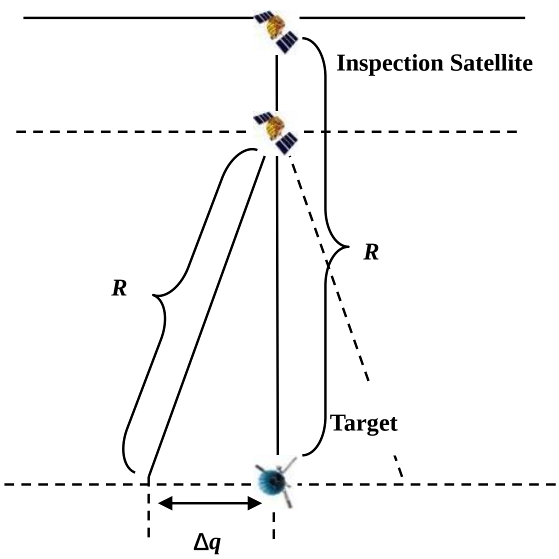

Figure 10. Schematic diagram of a certain sub-satellite point longitude threshold.

Set the point longitude threshold to Δq. The same remainder condition is trans-formed into

$$q_{D_i} = \{\lambda_i \in Z \quad \lambda_j \in Z \quad |\mathrm{mod}(\lambda_i^* \quad D_i) - \mathrm{mod}(\lambda_j^* \quad D_i)| \le \Delta q\} \tag{33}$$

Preprints.org (www.preprints.org) | NOT PEER-REVIEWED | Posted: 10 February 2025 doi:10.20944/preprints202502.0677.v1

Correspondingly, the target set corresponding to the mode becomes the target set corresponding to the same set of residues with the most elements

$$Q_D = \left\{ q_D \left| num(q_D) = \max\left(num\left(q_{D_i}\right)\right) \right. \right\} \tag{34}$$

Take the intersection of the target set Q generated by each longitude drift rate mentioned above, and find two sets of longitude drift rates, which are the east-west longitude drift rates used by the satellite for patrol.

2.5. Determine the Starting Position of Patrol for Each Region

Assuming that the set of eastward drift targets and westward drift targets are Q_E and Q_W, the initial position λ_E and λ_W is

$$\begin{aligned} \lambda_E &= \min(Q_E) - p_E D_E \\ \lambda_W &= \max(Q_W) + p_W D_W \end{aligned} \tag{35}$$

And p_E and p_W meet

$$\begin{aligned} &\min(Q_E) - p_E D_E \le \min(Z_i) \le \min(Q_E) - p_E D_E + D_E \\ &\max(Q_W) + p_W D_W - D_W \le \max(Z_i) \le \max(Q_W) + p_W D_W \end{aligned} \tag{36}$$

At this point, the initial time T_E of the eastward drift is the 0 o'clock of λ_E local time, and the initial time T_W of the westward drift is the 12 o'clock of λ_W local time.

2.6. Determine the Transfer Trajectory for Each Region

Assuming that the patrol satellite does not consume fuel during the westward and eastward drifts (ignoring the pulses applied during orbit maintenance), the classic double pulse orbit transfer method is used for the turning process. Eastward drift first and then westward, as shown in Figure 11.

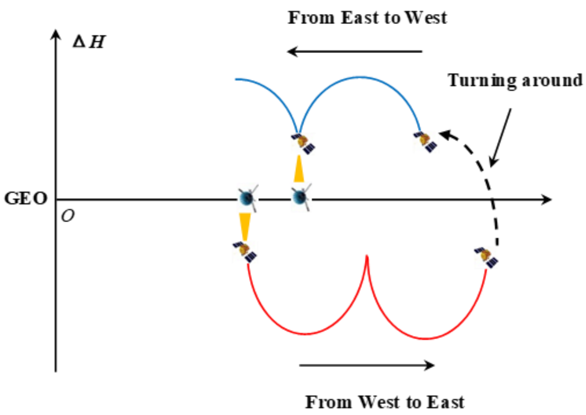

Figure 11. Schematic diagram of turning around.

From the previous section, it can be seen that when patrol satellite turns around from east drift to west drift, it should maneuver from the apogee of east drift orbit to the perigee of west drift orbit. As previously analyzed, the patrol position of eastward drift orbit is apogee, while the position of westward drift orbit is perigee, and the period is approximately 24 hours. The above transfer orbit allows the patrol satellite to carry out normal missions after turning around. The specific transfer process is shown in Figure 12.

Preprints.org (www.preprints.org) | NOT PEER-REVIEWED | Posted: 10 February 2025 doi:10.20944/preprints202502.0677.v1

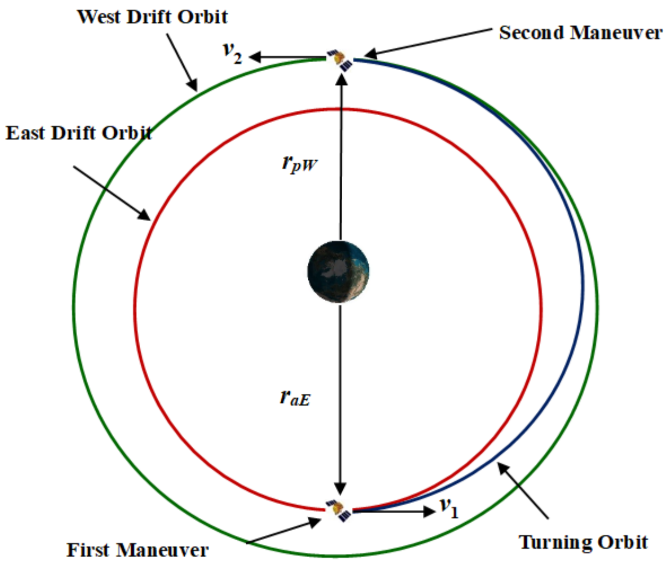

Figure 12. Schematic diagram of turning around orbit.

According to formula (1), the semi-major axes of east and west drift orbit are

$$a_E = a_c - \frac{D_E}{0.0128}$$
$$a_W = a_c + \frac{D_W}{0.0128} \quad (37)$$

The perigee of the transfer orbit is the eastward drift orbit apogee r_{aE}, and the apogee of the transfer orbit is the westward drift orbit perigee r_{pW}, then its semi-major axis is

$$a_T = \frac{r_{aE} + r_{pW}}{2} \quad (38)$$

Based on orbital knowledge, it is easy to obtain the velocity of the eastward drift orbit apogee v_{aE}, and the velocity of westward drift orbit apogee v_{pW}, and v_1 and v_2 of the transfer orbit apogee, respectively

$$v_{aE} = \sqrt{\frac{\mu}{a_E}\frac{r_{pE}}{r_{aE}}}$$
$$v_{pW} = \sqrt{\frac{\mu}{a_W}\frac{r_{aW}}{r_{pW}}}$$
$$v_1 = \sqrt{\frac{\mu}{a_T}\frac{r_{pW}}{r_{aE}}}$$
$$v_2 = \sqrt{\frac{\mu}{a_T}\frac{r_{aE}}{r_{pW}}} \quad (39)$$

Therefore, the energy consumption required for the transition is

$$\Delta v_{EW} = v_1 - v_{aE} + v_{pW} - v_2 \quad (40)$$

Similarly, when the patrol satellite transitions from a west to east, it shifts from the perigee of the westward drift orbit to the apogee of the eastward drift orbit, as shown in Figure 13.

Preprints.org (www.preprints.org) | NOT PEER-REVIEWED | Posted: 10 February 2025 doi:10.20944/preprints202502.0677.v1

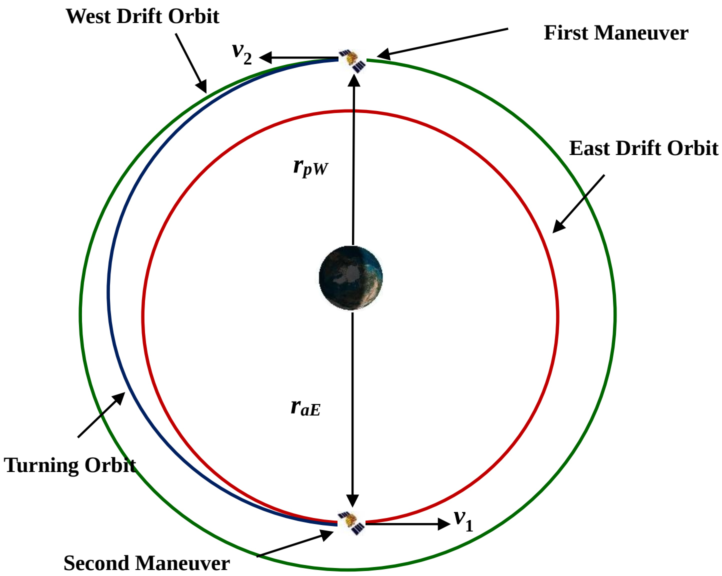

Figure 13. Schematic diagram of turning around orbit.

It can be seen that the required energy consumption is also

$$\Delta v_{WE} = v_1 - v_{aE} + v_{pW} - v_2 \quad (41)$$

Thus, it can be obtained that the energy consumption of patrol of the targets in the zone once is

$$\Delta V = \Delta v_{EW} + \Delta v_{WE} \quad (42)$$

3. Results

GEO satellites can be divided into three categories: military, civilian/government, and commercial. According to UCS database, there are a total of 48 IGSO military targets. In our paper, the analysis and design of patrol orbit configurations will be carried out for these targets. Based on the above steps, this section provides a specific analysis of the patrol for IGSO targets.

3.1. Calculate the Crossing Position and Crossing Time of the igso Targets

The crossing time of IGSO targets, and the results are shown in Table 1.

Table 1. The time of crossing the target.

NORAD Number	Time （UTCG）	NORAD Number	Time （UTCG）	NORAD Number	Time （UTCG）
23467	17:03:00	27168	15:57:00	41724	14:42:00
41937	22:45:00	26694	12:00:00	41940	10:06:00
43162	15:21:00	39120	13:54:00	38352	17:49:20
25019	13:01:20	43700	15:37:20	28158	11:58:20
38254	23:37:20	22787	14:06:00	44337	19:45:10
37481	11:03:00	28542	17:54:00	44204	11:29:00
27711	8:03:00	25639	16:36:00	37256	15:19:20
26715	13:27:00	38091	15:46:20	37804	11:01:20
22988	12:27:00	26880	8:31:20	37234	13:07:20
26695	8:42:00	39375	19:03:00	37377	21:06:00
33055	8:42:00	28117	12:54:00	44231	5:23:00
20253	22:37:20	25967	19:06:00	41586	0:25:20
38466	15:51:00	39234	5:48:00	43683	21:04:20
20776	13:12:00	29155	4:00:00	36287	9:07:20
44481	8:03:30	38953	15:19:20	37210	19:52:20
24737	15:46:20	42949	21:27:00	25258	17:54:00

Preprints.org (www.preprints.org) | NOT PEER-REVIEWED | Posted: 10 February 2025 doi:10.20944/preprints202502.0677.v1

3.2. Design the Spiral Trajectory That Satisfies Desired Patrol Time

The closer the observation distance, the more detailed characteristic information can be obtained. Therefore, when the distance between patrol satellite and GEO is the smallest, the observation effect is the best. That is, the observation position should be selected as the apogee (east drift orbit) or perigee (west drift orbit) of the patrol satellite. It can be seen that the conditions for forming a spiral ring are that the apogee velocity is less than the target orbit, while the perigee velocity is greater than the target orbit, that is

$$\begin{gathered} v_a \le v_c \\ v_p \ge v_c \end{gathered} \tag{43}$$

Among them, v_c is the reference orbit velocity, and v_a and v_p are the perigee and apogee velocities of the patrol orbit, respectively.

According to orbital dynamics, the velocities of the perigee and apogee can be expressed as

$$\begin{aligned} v_a &= \sqrt{\frac{\mu}{r_p + r_a}}\sqrt{\frac{2r_p}{r_a}} \\ v_p &= \sqrt{\frac{\mu}{r_p + r_a}}\sqrt{\frac{2r_a}{r_p}} \\ v_c &= \sqrt{\frac{\mu}{a_c}} \end{aligned} \tag{44}$$

By substituting into formula (19), we can obtain:

$$\frac{r_p\left(r_p + r_a\right)}{2r_a} \le a_c \le \frac{r_a\left(r_p + r_a\right)}{2r_p} \tag{45}$$

As analyzed above, the edge of the GEO maneuvering area is ± 75km, and the observation position is taken as perigee (west drift) or apogee (east drift), as shown in Figure 14.

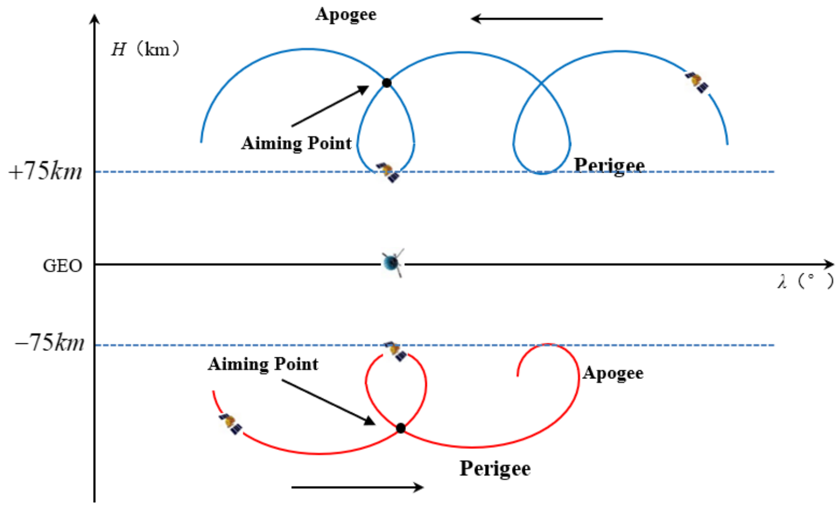

Figure 14. Schematic diagram of observation positions for patrol satellite.

$$\begin{aligned} &\text{East} \quad \frac{r_p\left(r_p + a_c - 75\right)}{2\left(a_c - 75\right)} \le a_c \le \frac{\left(a_c - 75\right)\left(r_p + a_c - 75\right)}{2r_p} \\ &\text{West} \quad \frac{\left(a_c + 75\right)\left(a_c + 75 + r_a\right)}{2r_a} \le a_c \le \frac{r_a\left(a_c + 75 + r_a\right)}{2\left(a_c + 75\right)} \end{aligned} \tag{46}$$

By organizing the above equation, we can obtain:

Preprints.org (www.preprints.org) | NOT PEER-REVIEWED | Posted: 10 February 2025 doi:10.20944/preprints202502.0677.v1

$$\begin{aligned} &\text{East drift} \quad a_c - a \geq \frac{150a_c}{a_c + 75} \\ &\text{West drift} \quad a - a_c \geq \frac{150a_c}{a_c - 75} \end{aligned} \tag{47}$$

By rearranging formulas (45) to (47), the relationship between the aiming point position, spiral ring period, and longitude drift rate D can be obtained as follows:

$$R = \begin{cases} 2\left(2a_c - \dfrac{2a_c^{\,2}}{2a_c - \dfrac{D}{0.0128}}\right) + 75 - a_c & r < a_c \\ 2\left(2a_c - \dfrac{2a_c^{\,2}}{2a_c - \dfrac{D}{0.0128}}\right) - 75 - a_c & r > a_c \end{cases} \tag{48}$$

$$T_s = 2\sqrt{\frac{a_c^{\,3}}{\mu}}\sqrt{\left(1 + \frac{-\dfrac{D}{0.0128}}{a_c}\right)^3}\left[\arccos\left(\frac{a\left(-\dfrac{D}{0.0128}\right)}{(a_c + a)\left(\dfrac{D}{0.0128} - 75\right)}\right) + \frac{\dfrac{D}{0.0128} - 75}{a}\sin\left(\arccos\left(\frac{a\left(\dfrac{D}{0.0128}\right)}{(a_c + a)\left(\dfrac{D}{0.0128} - 75\right)}\right)\right)\right] \tag{49}$$

The aiming point position and spiral ring period with respect to the longitude drift rate are shown in Figure 15 and 16.

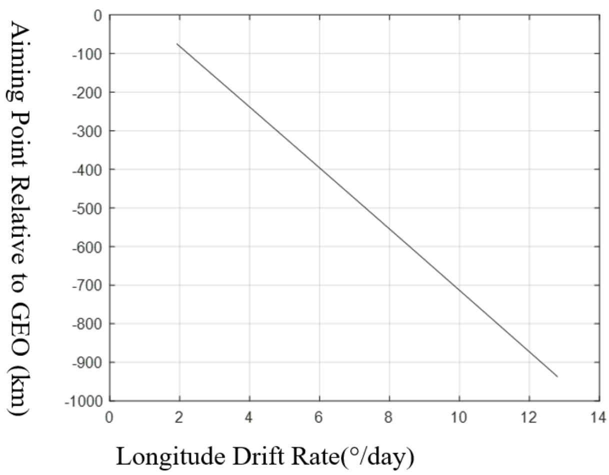

(a) Eastward drift

 doi:10.20944/preprints202502.0677.v1

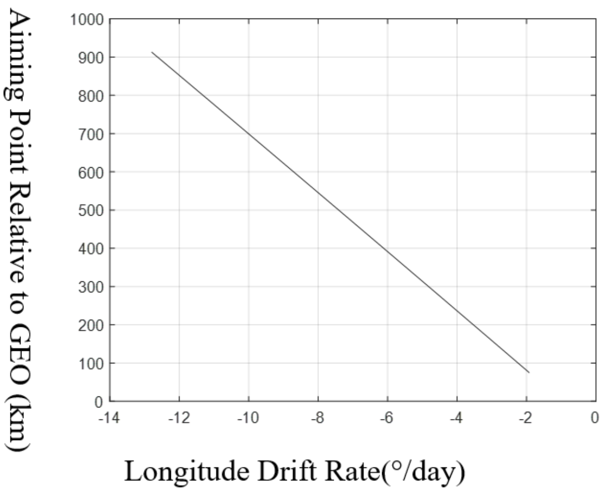

(b) Westward drift

Figure 15. Diagram of the aiming point position relative to GEO with longitude drift rate.

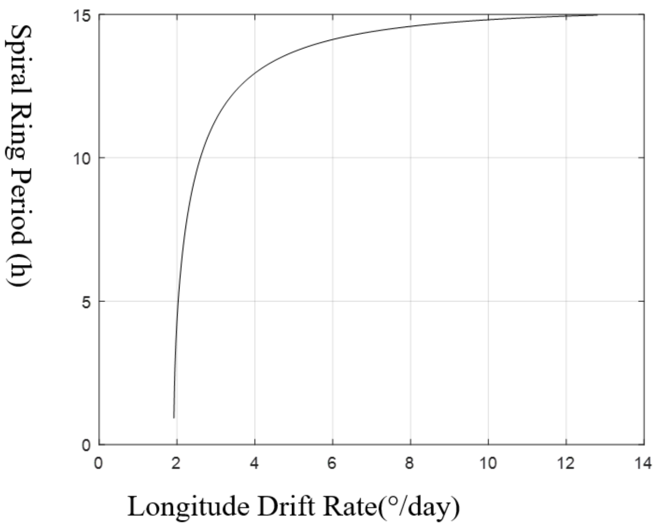

Figure 16. Diagram of spiral ring period variation with longitude drift rate.

3.3. Divide IGSO Targets into Regions Based on Dichotomy Approach

Use the dichotomy approach to divide the regions of 48 IGSO targets. There are several significant longitude gaps in the distribution of the targets. If the divided region covers these gaps, there may be a significant increase in the patrol period due to a certain target. Therefore, when dividing regions, it is important to avoid these gaps as much as possible. The position and the longitude difference gap for IGSO targets are shown in Table 2.

Table 2. IGSO targets position and its longitude difference.

Fixed-Point Longitude	-177.1	-159.6	-159.0	-130.1	-120.0	-96.8	-90.0
Longitude Difference	17.5	0.6	28.9	10.1	23.2	6.8	
Fixed-Point Longitude	-90.0	-67.9	-38.9	-34.0	-17.8	-14.7	-10.1
Longitude Difference	22.1	29	4.9	16.2	3.1	4.6	
Fixed-Point Longitude	-10.1	-1.3	0.0	3.9	16.3	20.6	26.0
Longitude Difference	8.8	1.3	3.9	12.4	4.3	5.4	
Fixed-Point Longitude	26.0	28.8	29.0	35.6	59.0	69.5	70.0
Longitude Difference	2.8	0.2	6.6	23.4	10.5	0.5	
Fixed-Point Longitude	70.0	71.5	72.7	74.0	75.0	80.0	91.1
Longitude Difference	1.5	1.2	1.3	1.0	5.0	11.1	
Fixed-Point Longitude	91.1	92.0	93.1	98.0	103.8	106.0	113.9
Longitude Difference	0.9	1.1	4.9	5.8	2.2	7.9	
Fixed-Point Longitude	113.9	118.0	129.8	130.0	131.1	143.0	144.0
Longitude Difference	4.1	11.8	0.2	1.1	11.9	1.0	
Fixed-Point Longitude	144.0	144.5	160.0	172.3	-177.1		
Longitude Difference	0.5	15.5	12.3	10.6			

From Table 2, it can be seen that there are 5 longitude differences greater than 20 °, but the first four notches are very concentrated, considering the actual situation such as period. Mark the longitude gaps greater than 10 °, and control the patrol period of each region to be within 60 days. Based on the distribution characteristics of IGSO targets and the analysis of orbital longitude drift rate, the targets are divided into 7 regions. The division is shown in Table 3.

Table 3. IGSO targets division.

Area Number	A	B	C	D	E	F	G
Crossing Targets	160.0	-130.1	-38.9	16.3	59.0	91.1	129.8
	172.3	-120.0	-34.0	20.6	69.5	92.0	130.0
	-177.1	-96.8	-17.8	26.0	70.0	93.1	131.1
	-159.6	-90.0	-14.7	28.8	71.5	98.0	143.0
	-159.0	-67.9	-10.1	29.0	72.7	103.8	144.0
			-1.3	35.6	74.0	106.0	144.5
			0.0		75.0	113.8	
			3.9		80.0	118.0	

3.4. Calculate the Bidirectional Longitude Drift Rate Within Each Region

As shown in the Figure4, as longitude drift rate increases, the aiming point position relative to GEO increases linearly. As shown in the Figure5, the spiral ring period shows a rapid growth and then a slowing trend, eventually tending towards 15 hours. If the crossing time is all corresponded to the interval range of 0-12 hours (according to the concept of crossing points, crossing points always appear in pairs, and there must be a crossing point in this interval), and the patrol satellite adopts a strategy of regional control and round-trip. To achieve comprehensive coverage of crossing time, it requires that the spiral ring period cannot be less than 12 hours. According to Figure 5, the longitude drift rate corresponding to a 12 hour is 3.3 °/day.

On the other hand, in order to ensure that patrol satellite can observe the target during the spiral loop, the position of the aiming point relative to GEO needs to meet the observation distance constraint condition, which is less than 250km. Similarly, as shown in Figure5, the longitude drift rate

 doi:10.20944/preprints202502.0677.v1

corresponding to a relative distance of 250km is 4.1 °/day. In summary, the longitudinal drift rate of the patrol orbit for IGSO targets is:

$$\begin{aligned} &\text{East drift inspection} \quad 3.3 \le D \le 4.1 \\ &\text{West drift inspection} \quad -4.1 \le D \le -3.3 \end{aligned} \tag{50}$$

Also consider setting region thresholds for the target set:

$$\Delta q = 0.2^{\circ} \tag{51}$$

At this point, the corresponding aiming point position is 200km. As shown in Figure 4, the corresponding longitude drift rate is 3.5 °/day. Therefore, the set of longitude drift rates D is:

$$\begin{aligned} &\text{East drift inspection} \quad 3.3 \le D \le 3.5 \\ &\text{West drift inspection} \quad -3.5 \le D \le -3.3 \end{aligned} \tag{52}$$

The above calculation is applied to each region using the gradient longitude drift rate strategy, and the longitude drift rate and patrol period for each region were obtained as shown in Table 4. From the table, it can be seen that the longest period does not exceed 40 days.

Table 4. Longitude drift rate and patrol period of geo crossing target regions.

Region	A	B	C	D	E	F	G
Drift Rate of Westward Drift(°)	3.4	3.4	3.4	3.4	3.5	3.4	3.3
Drift Rate of Eastward Drift(°)	3.5	3.4	3.5	3.3	3.5	3.4	3.3
Traverse Cycle (Day)	25	39	28	13	14	18	12

3.5. Determine the Starting Position of Patrol for Each Region

The initial positions of the west drift and east drift are shown in Table 5.

Table 5. The initial positions of each region.

Region	A	B	C	D	E	F	G
Initial Longitude Value of East Drift	158.4	-130.2	-39.0	16.1	58.9	91.0	129.8
Initial Longitude Value of West Drift	-159	-66	6.8	35.6	82.0	120.6	147.6

3.6. Determine the Transfer Trajectory for Each Region

The fuel consumption for one patrol cycle in each region can be obtained as shown in Table 6. It can be seen that the energy consumption does not exceed 0.04km/s. The total energy consumption of a single patrol cycle in all regions shall not exceed 0.272km/s.

Table 6. Energy consumption for one patrol cycle.

Region	A	B	C	D	E	F	G
ΔV	0.0393	0.0387	0.0393	0.0382	0.0399	0.0387	0.0376

In summary, the IGSO patrol configuration designed in this article is shown in Figure 17.

Preprints.org (www.preprints.org) | NOT PEER-REVIEWED | Posted: 10 February 2025 doi:10.20944/preprints202502.0677.v1

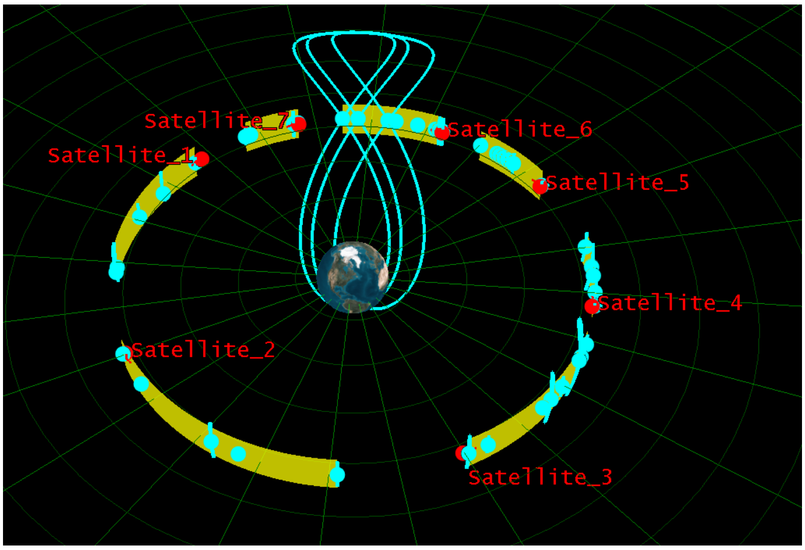

Figure 17. Schematic diagram of the IGSO patrol configuration.

4. Discussion

Taking zone A as example, there are 5 targets in this region, with sub-satellite point longitudes of {-160.0, 172.3, -177.1, -159.6, -159.0}, and the longitude drift rate used is

$$\begin{aligned} D_E &= 3.5 \\ D_W &= 3.4 \end{aligned} \tag{53}$$

The corresponding sets of east and west drift targets are

$$\begin{aligned} Q_E &= \{172.3 \quad -177.1 \quad -159.6\} \\ Q_W &= \{160.0 \quad -159.0\} \end{aligned} \tag{54}$$

The corresponding initial positions for east and west drift are

$$\begin{aligned} \lambda_E &= 158.4 \\ \lambda_W &= -159.0 \end{aligned} \tag{55}$$

The simulation results are shown in Figure 18.

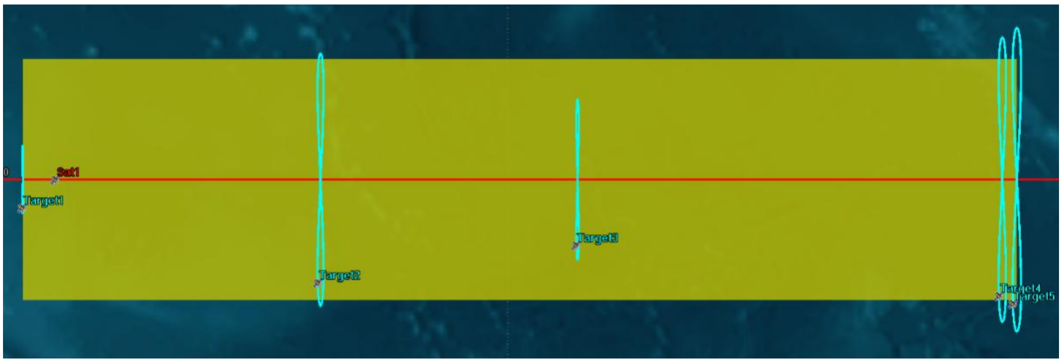

(a) 2D Result

Preprints.org (www.preprints.org) | NOT PEER-REVIEWED | Posted: 10 February 2025 doi:10.20944/preprints202502.0677.v1

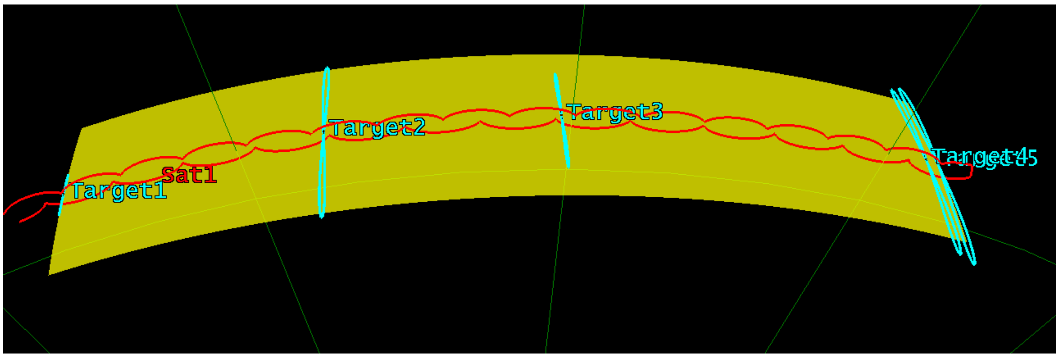

(b) 3D Result

Figure 18. Patrol simulation results of zone A.

It can be seen that the patrol satellite has achieved patrol of all targets. The patrol of various targets is shown in Figure 19.

Preprints.org (www.preprints.org) | NOT PEER-REVIEWED | Posted: 10 February 2025 doi:10.20944/preprints202502.0677.v1

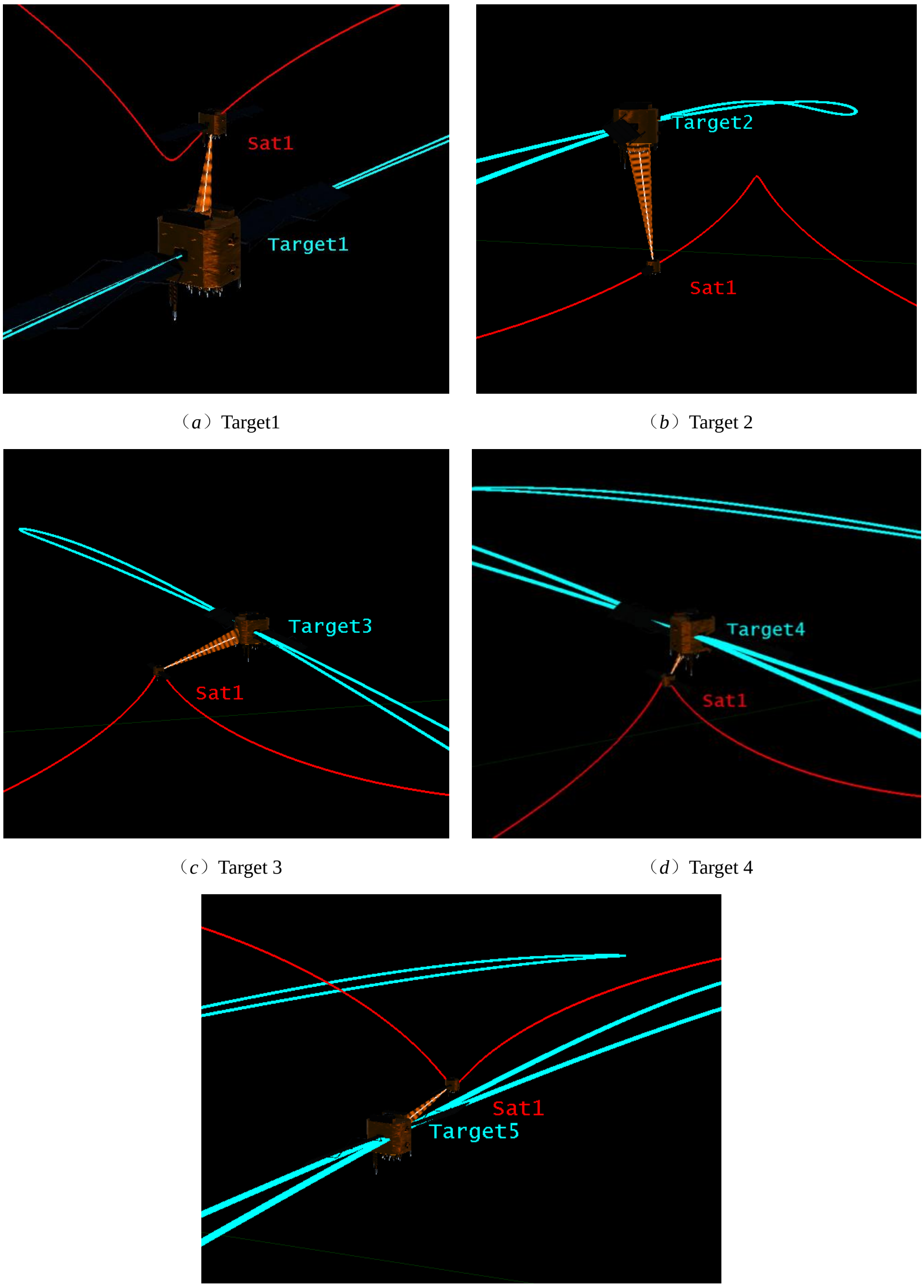

（*a*） Target1 （*b*） Target 2

（*c*） Target 3 （*d*） Target 4

（*e*） Target 5

Figure 19. Patrol of various targets by patrol satellite.

During the patrol, the minimum observation distance and observation duration of the satellite for each target are shown in Table 7.

Table 7. The minimum observation distance and duration for each target.

Target	1	2	3	4	5
Minimum observation distance （km）	108.8	187.1	205.7	84.7	101.1
Observation duration （s）	5820.6	1180.5	1585.7	1487.6	1352.9

From Table 7, it can be seen that for region A, the minimum observation distance of the patrol satellite for each target is less than 250km, and the observation duration that meets the observation condition constraint is above 20 minutes, which can ensure the patrol of targets.

5. Conclusions

This paper focuses on the patrol of IGSO targets. A method based on step longitude drift rate and crossing points is proposed for patrol IGSO targets, includes: (1) Calculate the crossing position and crossing time of the IGSO targets; (2) Design the spiral trajectory that satisfies desired patrol time; (3) Divide IGSO targets into regions based on dichotomy approach; (4) Calculate the bidirectional longitude drift rate within each region; (5) Determine the starting position of patrol for each region; (6) Determine the transfer trajectory for each region. Using the above methods, STK tool was used to simulate target in region A, and the simulation results verified that using the gradient longitude drift rate method based on crossing points and spiral rings can achieve patrol of IGSO targets. The patrol period shall not exceed 40 day, and an energy consumption of no more than 0.04km/s for a single zone patrol period. The total energy consumption of a single patrol cycle in all zones shall not exceed 0.272 km/s. The approach proposed in this article not only can be applied in the design of GEO Zone patrol route, but also be used to guide Space Traffic Patrol, thereby enhancing Space safety.

6. Patents

This work was supported by National Defense Science and Technology Excellence Youth Fund Project of China. And, all data, models, and code generated or used during the study appear in the submitted paper.

References

1. Quan Haofang, Li Xiaolong. Preliminary Research on Space Traffic Management Standards System [J]. Space Debris Research, 2021, Volume 21 (81): 50-57.
2. Duan Feng. Research on the Shift from Space Traffic Management to Space Traffic Coordination in the United States [J]. Space Debris Research, 2022, Volume 22 (83): 66-71.
3. Yao Wenduo, Feng Shuxing, Chen Lingyun. Study on the Development of Space Traffic Management[J]. Aerospace China, 2021(3): 49-52.
4. Feng Shuxing, Yao Wenduo, Chen Lingyun. Discussion on the Framework of Space Traffic Management System[J]. Aerospace China, 2021(9): 38-43.
5. Space Debris Mitigation Guidelines. IADC, Revision 2, 2020.
6. ESA's Annual Space Environment Report. ESA, 2024.
7. https://www.ucsusa.org/resources/satellite-database
8. Haijun Shen and Panagiotis Tsiotras. Optimal Scheduling for Servicing Multiple Satellites in a Circular Constellation[C]. AIAA/AAS Astrodynamics Specialist Conference and Exhibit, Monterey, California, August 5~8,2002.
9. Alfriend K T, Creamer N G, Lee D J. Optimal Servicing of Geosynchronous Satellites[J]. Journal of Guidance Control and Dynamics, 2006, 29(1):203-206.
10. Zhou Y, Yan Y, Huang X, et al. Mission planning optimization for multiple geosynchronous satellites refueling[J]. Advances in Space Research, 2015, 56(11):2612-2625.
11. Xu Yanli, Zhang Yasheng. Design and Simulation of Spiral Cruise Orbit[C]. System Simulation Technology and Its Application.
12. Zheng Letian, Xu Yanli, Zhu Dongjun. Cruise orbit design for multiple geostationary orbit targets[J]. Aerospace Control and Application, 2016, 42(5):37-41.
13. Bo X, Feng Q. Research on constellation refueling based on formation flying[J]. Acta Astronautica, 1987, 68(11-12):1987-1995.
14. Huang, Xu, Yan, et al. Optimal scheduling of multiple geosynchronous satellites refueling based on a hybrid particle swarm optimizer[J]. Aerospace Science & Technology, 2015, 47:125-134.

15. Madakat D, Morio J, Vanderpooten D. Biobjective planning of an active debris removal mission[J]. Acta Astronautica, 2013, 84(MAR.-APR.):182-188.
16. Du B, Zhao Y, Dutta A, et al. Optimal scheduling of multisatellite refueling based on cooperative maneuver[J]. Advances in Space Research, 2015, 55(12):2808-2819.
17. Jackson B. Minimum energy maneuvering strategies for multiple satellite inspection missions[C]. Aerospace Conference, IEEE, 2005.
18. Zhang J, Parks G T, Luo Y Z, et al. Multisatellite Refueling Optimization Considering the J2 Perturbation and Window Constraints[J]. Journal of Guidance Control & Dynamics, 2014, 37(1):111-122.
19. Zhou Y, Yan Y, Huang X, et al. Optimal scheduling of multiple geosynchronous satellites refueling based on a hybrid particle swarm optimizer[J]. Aerospace Science and Technology, 2015, 47:125-134.
20. Zhang T J, Shen H X, Wang B H, et al. Optimal scheduling for location geosynchronous satellites refueling problem[J]. Acta Astronautica, 2019.
21. Haijun Shen and Panagiotis Tsiotras. Peer-to-Peer Refueling for Circular Satellite Constellations[J]. Journal of Guidance Control & Dynamics, 2005.
22. Salazar A, Tsiotras P. An auction algorithm for allocating fuel in satellite constellations using peer-to-peer refueling[J]. 2006.
23. Chen X Q, Yu J. Optimal mission planning of GEO on-orbit refueling in mixed strategy[J]. Acta Astronautica, 2017, 133(apr.):63-72.
24. Atri Dutta∗, Panagiotis Tsiotras†. Asynchronous optimal mixed P2P satellite refueling strategies[J]. The Journal of the Astronautical sciences, 2006, 54(3-4):543-565.
25. Xiao Dongdong, Xu Bo, Gao Youtao, etc Optimization of Supply Orbit for Heterogeneous Constellations Based on Companion Flight Mode [J] Chinese Science: Physics, Mechanics, Astronomy, 2012 (12): 67-77.
26. Xiao Dongdong, Zhu Qinghua, Zu Liye Research on Multi Supply Tasks of Heterogeneous Constellations Based on Accompanying Flight Mode [J] Shanghai Aerospace, 2016, 33 (02): 9-14
27. Zhang T J, Shen H X, Wang B H, et al. Optimal scheduling for location geosynchronous satellites refueling problem[J]. Acta Astronautica, 2019, 163:264-271.
28. Yu J, Yu Y G, Hao D, et al. Biobjective mission planning for geosynchronous satellites on-orbit refueling[J]. Proceedings of the Institution of Mechanical Engineers, 2019, 233(2):686-697.
29. C. Prodhon, C. Prins. A survey of recent research on location-routing problems[J]. European Journal of Operational Research, 2014, 238:1–17.
30. Haijun Shen and Panagiotis Tsiotras. Peer-to-Peer Refueling for Circular Satellite Constellations[J]. Journal of Guidance Control & Dynamics, 2005, 28(6):1220-1238.
31. Salazar A, Tsiotras P. An auction algorithm for allocating fuel in satellite constellations using peer-to-peer refueling[C]. American Control Conference. IEEE, 2006.
32. B.L. Rui, C. Ferreira, B.S. Santos. A simple and effective evolutionary algorithm for the capacitated location routing problem[J]. Computers & Operation Research. 2016, 70: 155–162.
33. Dutta A, Tsiotras P. An Egalitarian Peer-to-Peer Satellite Refueling Strategy[J]. Journal of Satellite and Rockets, 2008, 45(3):608-618.
34. Dutta, A, and Tsiotras, P. Greedy Random Adaptive Search Procedure for Optimal Scheduling of P2P Satellite Refueling[C] AAS/AIAA Space Flight Mechanics Meeting, American Astronautical Society Paper 07-150, Jan. 2007.
35. Dutta, A, and Tsiotras, P. Network Flow Formulation for an Egalitarian P2P Refueling Strategy[C] AAS/AIAA Space Flight Mechanics Meeting, American Astronautical Society Paper 07-151, Jan. 2007.
36. Chen X Q, Yu J. Optimal mission planning of GEO on-orbit refueling in mixed strategy[J]. Acta Astronautica, 2017, 133(4):63-72.
37. Bai Xiaozheng, Xi Xiaoning Realizing close proximity between a single spacecraft and multiple satellites in a constellation without the need for orbit changes [J] Journal of Astronautics, 2005, 026 (0z1): 114-116.
38. Wang Wei, Huang Wende, Fu Xiaofeng, etc The close-up approach of a single spacecraft to multiple satellites in the Walker constellation [J] Journal of Space Science, 2005, 25 (006): 547-551
39. Tang Rong, Wang Wei, Fu Xiaofeng Orbit selection and optimization for approaching multiple Walker constellation satellites [J] Computer Simulation, 2008 (04): 59-62.

 doi:10.20944/preprints202502.0677.v1

40. Zhang Jing, Xi Xiaoning, Wang Wei Sufficient conditions and characteristic analysis for a single spacecraft to rendezvous with multiple stars in the Walker constellation without the need for orbit change [J] Journal of National University of Defense Technology, 2010, 32 (6): 87-92.
41. Zhang Jing, Wang Wei, Xi Xiaoning Approach orbit design for deviated Walker constellation satellites [J] Journal of Astronautics, 2008, 29 (4): 1200-1204.
42. Zhang Jing, Wu Meiping, Fu Xiaofeng The Application of Genetic Algorithm in Optimization of Multi star Approach Orbits in Constellations [J] Journal of Space Science, 2012, 32 (001): 99-105.
43. Yang Yidai Research on Satellite Traverse Target Dynamics and Orbit Design Problems [D] Harbin Institute of Technology, 2012.
44. Mana. Fuel optimal orbit design for satellite constellation traversal in limited thrust mode [D] Harbin Institute of Technology, 2017.
45. Zhang Yasheng, Zhou Haijun A multi-objective rendezvous orbit design method based on crossing points [J] Modern Defense Technology, 2013 (05): 13-17.
46. Li Yuanfei, Zhang Yasheng Design of non-coplanar multi-objective rendezvous orbits based on crossing points [J] Aerospace Control, 2013, 31 (6): 66-70.
47. Zhang Y , Xu Y , Zhou H .Theory and Design Methods of Special Space Orbits[M].Springer Singapore,2017.